

# SuperScaler: Supporting Flexible DNN Parallelization via a Unified Abstraction

Zhiqi Lin<sup>†,‡,\*</sup>, Youshan Miao<sup>‡</sup>, Guodong Liu<sup>§,‡,\*</sup>, Xiaoxiang Shi<sup>¶,‡,\*</sup>, Quanlu Zhang<sup>‡</sup>, Fan Yang<sup>‡</sup>,  
Saeed Maleki<sup>‡</sup>, Yi Zhu<sup>‡</sup>, Xu Cao<sup>‡</sup>, Cheng Li<sup>†</sup>, Mao Yang<sup>‡</sup>, Lintao Zhang<sup>‡</sup>, Lidong Zhou<sup>‡</sup>

<sup>†</sup>University of Science and Technology of China, <sup>‡</sup>Microsoft Research,

<sup>§</sup>Institute of Computing Technology, Chinese Academy of Sciences, <sup>¶</sup>Shanghai Jiao Tong University

## Abstract

With the growing model size, deep neural networks (DNN) are increasingly trained over massive GPU accelerators, which demands a proper parallelization plan that transforms a DNN model into fine-grained tasks and then schedules them to GPUs for execution. Due to the large search space, the contemporary parallelization plan generators often rely on empirical rules that couple transformation and scheduling, and fall short in exploring more flexible schedules that yield better memory usage and compute efficiency. This tension can be exacerbated by the emerging models with increasing complexity in their structure and model size.

SuperScaler is a system that facilitates the design and generation of highly flexible parallelization plans. It formulates the plan design and generation into three sequential phases explicitly: model transformation, space-time scheduling, and data dependency preserving. Such a principled approach decouples multiple seemingly intertwined factors and enables the composition of highly flexible parallelization plans. As a result, SuperScaler can not only generate empirical parallelization plans, but also construct new plans that achieve up to 3.5× speedup compared to state-of-the-art solutions like DeepSpeed, Megatron and Alpa, for emerging DNN models like Swin-Transformer and AlphaFold2, as well as well-optimized models like GPT-3.

## 1 Introduction

The size of deep neural network (DNN) has grown significantly [8, 13, 30] over the past few years and the trend clearly shows little sign of any slow down. Accelerators such as GPUs are crucial for training such models thanks to the compute power they offer. However, single GPU’s memory has not scaled as fast as the model sizes. Large DNN models like GPT-3 [8] cannot fit into a single accelerator (*e.g.*, GPU) due to limited available memory. Therefore, utilizing parallel GPUs to distribute a model’s weights has become the main method to enable training of such large models. However, efficiency on a distributed GPU cluster is a major DNN system research problem.

Frameworks such as PyTorch [36] and TensorFlow [4] have simplified expressing the architecture of a DNN in terms of

basic operators such as matrix multiplication. Composing these operators creates a data flow graph (DFG) which is a directed acyclic graph (DAG) and each node is a basic operator and every edge corresponds to the data dependency between the source and the destination. A DNN framework takes the DFG as an input and computes the operators following DFG dependencies. For a given model, this DFG is executed numerous times each with a different input and the model weights are updated with every few iterations.

The corresponding DFG for a large model may have large operators and a large graph. Limited compute power and memory capacity of a single GPU dictates partitioning large operators into multiple smaller independent operators and then assigning them to different GPUs. We call the end-to-end scheme of partitioning and scheduling the DFG on multiple GPUs a *parallelization plan*.

Finding an optimal parallelization plan is the cornerstone of efficient DNN training. For example, one has to evaluate the trade-offs between a spatial scheduling that computes a DNN model on multiple GPUs concurrently to improve the degree of parallelism and a temporal scheduling that runs operators of the model in one GPU sequentially to save communication costs [20, 53]. Similarly, the granularity of operator aggregation and mapping them to pipeline stages on different GPUs [19, 28] is equally important to balance for optimal performance. At the same time, the plan should respect the original data dependency for correctness. In another word, the design of a parallelization plan requires a complex joint consideration of multiple intertwined factors: model partitioning, space-time scheduling (defining which GPU and when an operator executes), and data dependency preserving. To resolve this high complexity, existing systems support the parallel training of popular DNN models through predefined, well-studied parallelization plans composed by empirical parallelization rules, *e.g.*, tensor parallelism [20, 45] or pipeline parallelism [19, 50], or the combination of rules [34, 46, 61]. Such abstracted approaches show limited flexibility and do not work well on emerging DNN models like AlphaFold2 (§2).

This paper presents SuperScaler, a system that helps developers to design and generate highly flexible parallelization plans for deep learning training. Departed from empirical solutions, SuperScaler takes a principled approach that formulates the design of parallelization plan as three sequential

\*This work was done when the authors were with Microsoft Research.

phases explicitly: model partitioning, space-time scheduling, and data dependency materialization.

In the model partitioning phase, SuperScaler provides `op-trans`, a primitive that allows developer to express model partitioning as the transformation of each operator in the data flow graph representing the model. The developer can provide multiple legal transformations for one operator, and SuperScaler can compose them into graph-level transformation. Given a transformed graph (partitioned model), SuperScaler moves to the scheduling phase. It provides `op-assign` and `op-order` primitives for developers to express various space-time scheduling schemes, with `op-assign` mapping a portion of partitioned model to a certain GPU spatially, and `op-order` expressing a `happen-before` constraint to enforce the temporal execution order between operators without explicit data dependency. These two phases allow developers to consider transformation and scheduling, *separately* which enables the expression of highly flexible parallelization plans that existing solutions do not support (§3.4).

The flexibility enabled by the separation between model partitioning and scheduling may increase the burden of developers as the transformation and scheduling process could be error-prone. The transformation may require sophisticated changes in data dependencies to preserve the correct mapping between new and original graphs. For example, one may accidentally specify temporal scheduling order that violates data dependencies and leads to deadlocks. To address this problem, SuperScaler introduces `vTensor` to track the logical data dependencies before and after each operator transformation, and maintains the dependencies between transformed operators through the original data flow graph (§3.1). After scheduling decision is made, SuperScaler performs deadlock detection through the analysis of the tracked data dependency, alerts the developers of potential violation so that they can refine the design accordingly. The process repeats iteratively until no violation is detected. This facilitates the reasoning of various parallelization plans during the design process.

In the final phase, SuperScaler will automatically materialize the logical data dependency tracked during graph transformation and scheduling. The dependency materialization automatically inserts a collective communication primitive such as all-reduce for an operator that is split and scheduled across GPUs. These communication primitives can have unconventional semantics if two dependent operations are assigned to two different number of GPUs (§4). The automatic data dependency materialization and communication operation insertion further relieves developers from the tedious and error-prone process of exploring parallelization plans.

With the above design, SuperScaler decouples multiple seemingly intertwined factors and enables developers to design different parallelization plans without worrying about the underlying system implementation details.

SuperScaler is implemented based on PyTorch [36]. Developers use SuperScaler’s primitives, `op-trans`, `op-assign`

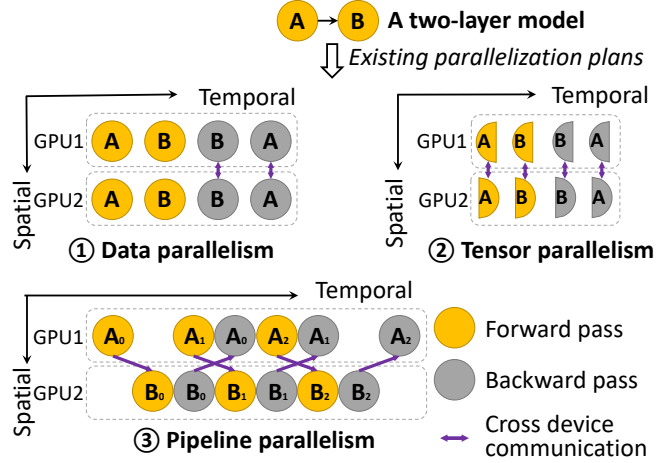


Figure 1: Empirical parallelization plans.  $A_i$  and  $B_i$  denote the computation on  $i$ -th micro-batch.

and `op-order`, to write `sProgram`, a program describing how a given DNN model, represented by a DFG, is transformed and scheduled. SuperScaler will then compile the `sProgram` into an execution flow graph served as an intermediate representation of the parallelization plan. SuperScaler analyzes this graph for automatic data dependency materialization and deadlocks detection. Finally, the resulting SuperScaler graph is compiled back into PyTorch codes for execution via PyTorch engine.

The flexibility of SuperScaler offers easy exploration of new parallelization plans such as co-shard and interlaced pipeline (§2) besides existing empirical plans. This is only possible by SuperScaler’s flexible space-time scheduling and materialization of data dependency leveraging unconventional communication patterns. The resulting parallelization plans are shown to achieve  $3.5\times$  speedup compared to state-of-the-art parallel training systems, including DeepSpeed [38], Megatron [34] and Alpa [61], for emerging DNN models in computer vision (Swin-Transformer [30]), language translation (mBART [29]), and biology analysis (AlphaFold2 [21]). Surprisingly, with the new parallelization plans SuperScaler can even achieve  $1.5\times$  speedup for well-optimized models like GPT-3 under certain realistic configurations. We plan to release SuperScaler to the open-source community.

## 2 Background and Motivation

**Empirical parallelization plans.** Today, parallel deep learning training mostly relies on parallelization plans composed by empirical rules. Figure 1 highlights several empirical parallelization plans. As most DNN models have multiple layers, *data parallelism* partitions all the layers to the same number of pieces along the batch dimension of the input tensor, the partitions are spatially placed on disjoint devices. Cross-partition communication only happens during the backward pass, a

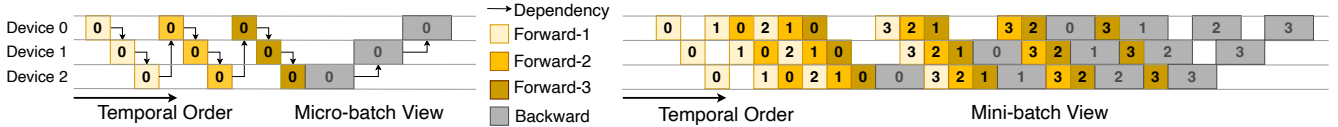


Figure 2: A specialized parallelization plan for AlphaFold.

computation executes in the reverse direction of the data dependency depicted in the model’s data flow graph, using the “all-reduce” primitive. Data parallelism assumes the whole model can fit in a single device, which is often not feasible for large models. Thus, *tensor parallelism* partitions a model (usually along an axis other than the batched dimension) evenly and places on disjoint devices. In tensor parallelism, cross-partition communication is complicated, it happens during both forward and backward passes, and requires different types of communication primitives (*e.g.*, all-reduce, reduce-scatter). This parallelization plan often introduces a large amount of communication. *Pipeline parallelism* can greatly reduce communication costs in some popular models (*e.g.*, BERT [14]). It groups layers of a model into several stages, each is placed on a dedicated device(s). The execution of each stage is temporally scheduled by pipelining the execution of multiple micro-batches, *i.e.*, splitting a mini-batch into multiple micro-batches, as shown in Figure 1. The communication across devices is peer-to-peer send/receive. Some improve the device utilization, some propose to improve the naive pipeline parallelism with more sophisticated temporal ordering across micro-batches (*e.g.*, 1F1B [50]). Moreover, the above empirical parallelization plans can be combined in a sequential and nested way, *i.e.*, pipeline parallelism with data or tensor parallelism applied within each pipeline stage [45, 56, 61], to further improve performance.

Although effective for popular DNN models, all these empirical parallelization plans couples model partitioning, space-time scheduling, and the corresponding changes in data dependency together. For example, both data and tensor parallelisms carefully align the communication primitives with the way the model is partitioned and assigned to disjoint devices. Pipeline parallelism requires careful temporal ordering to minimize device idle time, assuming stages are placed disjointly. This practice limits the flexibility of parallelization plans, as elaborated next.

**Emerging DNN models require new parallelization plans.** We observe that new DNN models have unique characteristics that existing parallelization plans cannot support effectively. For example, AlphaFold2 [21], the state-of-the-art model for molecular structure analysis, has three forward passes and one backward pass. As shown on the left of Figure 2, the output of each forward pass is the input of next pass, all the way to the backward pass. To effectively support AlphaFold2, the model needs to be trained in pipeline parallelism, but with a new temporal ordering specified for the micro-batches (shown on

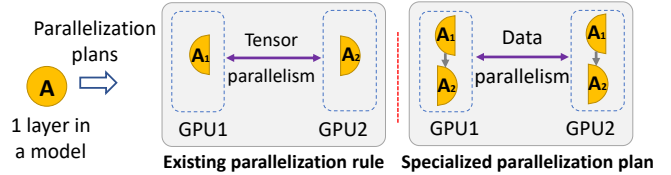


Figure 3: co-shard: a new parallelization plan.

the right of Figure 2). This new pipeline parallelism pattern (we call it 3F1B) cannot be expressed by any of the existing pipeline schemes. And to define a new rule for this pattern clearly lacks flexibility. This motivates us to design a new scheduling primitive for order preservation.

Another example is shown in Figure 3. This new parallelization plan, co-shard breaks the assumption that model partitions are required to be mapped to disjoint devices. The diagram on the right of Figure 3 shows that partitioned model can be placed to the same GPU and executed sequentially. This makes it possible to apply more communication efficient data parallelism across GPUs. In contrast, the traditional tensor parallelism could introduce higher communication cost. Co-shard is shown effective for Swin-Transformer [30], a new transformer for vision tasks. Co-shard partitions the model along its multi-head dimension [52], co-locates the partitioned model in one GPU, leveraging recompute [10] to reduce the peak memory usage, and achieves up to  $3.5\times$  speedup (§6).

§3.4 discusses some more examples. All these highlight the limitation of empirical parallelization plans and necessitate a system to facilitate the design of highly flexible parallelization plans.

### 3 Design

To support more flexible parallelization plans, SuperScaler allows developers to focus on model partitioning and space-time scheduling, while delegating the sophisticated, error-prone process of data dependency materialization to SuperScaler. Figure 4 summarizes the overall workflow of SuperScaler. The input of SuperScaler is a DNN model computation graph. Besides DNN model, developers also provide an sProgram that express a parallelization plan with primitives `op-trans`, `op-assign` and `op-order`. SuperScaler first exploits inherent parallel of DNN model by applying `op-trans` to partition operators into multiple functional equivalent operators. SuperScaler also tracks the data relations during model transformation (§3.1). Then, SuperScaler performs space-time schedul-

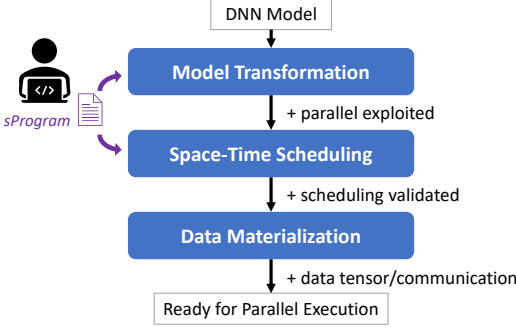


Figure 4: SuperScaler system workflow.

ing with primitive `op-assign` assigning each operator an execution device and `op-order` that enforces execution orders between operators. SuperScaler also builds data dependency from tracked data relation to validate scheduling and avoid possible deadlock (§3.2). Finally, SuperScaler materializes the tracked data dependency into communications that connect mismatched data partitioning and cross device operators, and generates parallel execution (§3.3).

### 3.1 Operator Transformation

DNN models, defined as operators performing computation over high dimensional tensor data, can be partitioned into finer-grain tasks to exploit parallelism. SuperScaler performs such operation over each operator with `op-trans`. Following a user-defined transformation algorithm `algo`, an `op-trans(op, algo)` partitions an operator `op` along with its input and output data tensors into a set of functional equivalent operators and tensors.

**vTensor.** SuperScaler introduces `vTensor` to track the changing data dependency during operator transformation. A `vTensor` “links” to a `pTensor`, which is a logically persistent tensor defined in the original DNN model (e.g., Figure 5). Besides the link, a `vTensor` also maintains a “mask”, representing which portion of the `pTensor` the operator accesses (e.g., Figure 6). Each operator has their own dedicated input and output `vTensors`, even multiple operators access the same `pTensor`. As shown on the top of Figure 5, operator A’s output data is operator B’s input. The two operators linked to the same `pTensor` through their own `vTensors`, respectively. Leveraging `vTensor`, a transformation algorithm in `op-trans` is defined as a graph substitution, which describing: 1) each new operator’s computation, e.g., `MatMul`, `Add`, and 2) how to partition original input and output `vTensors` to get new operators’ input and output `vTensors`. When applying an `op-trans`, SuperScaler will only partition `vTensors` and leave `pTensors` unchanged. And `op-trans` over an operator won’t affect other operators’ `vTensors`, as different operators have dedicated `vTensors`. As shown in Figure 5, applying `op-trans` on operator A only splits itself and its output `vTensor`, leaving operator B unchanged. Such

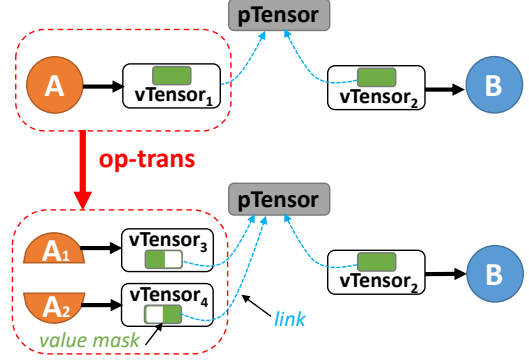


Figure 5: Perform `op-trans` on SuperScaler graph.

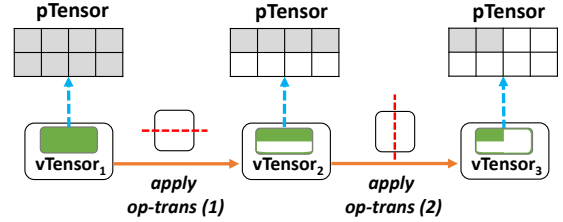


Figure 6: `vTensors` track data dependency during a series of `op-trans`.

separation allows developers to flexibly perform `op-trans` on different operators in `sProgram`. Moreover, developers do not need to align tensors between adjacent operators during transformation, e.g., aligning `vTensor3` and `vTensor4` with `vTensor2`, leaving such a tedious and error-prone process to the phase of data dependency materialization.

**Data dependency tracking through `vTensor`.** With `vTensor`, the link to `pTensor`, and the mask in a `vTensor`, SuperScaler can track data dependency during operator transformations. When `op-trans` partitions a `vTensor` into multiple `vTensors`, each new `vTensor` links to the same `pTensor` as the original `vTensor` but with a different mask. Figure 6 shows how SuperScaler tracks data dependency after two `op-trans`. In the process, `op-trans(1)` partitions the tensor horizontally, the resulting `vTensor2` maintains a mask atop to show it keeps the top half of `vTensor1` to the `pTensor`. `op-trans(2)` further partitions `vTensor2` vertically, turning it into `vTensor3`, whose mask indicates that the left half of `vTensor2`, which is the top-left part of `pTensor`. For two `vTensors` linked to the same `pTensor`, SuperScaler can easily detect whether they have data dependency by intersecting their masks. Such logical dependency will be used for space-time scheduling and dependency materialization.

### 3.2 Space-Time Scheduling

SuperScaler introduces `op-assign(op, device)` and `op-order(op1, op2)` to enable flexible space-time scheduling. For example, `op-assign(op1, GPU0)` assigns device

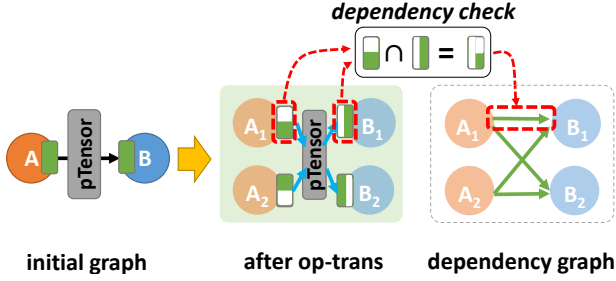


Figure 7: Checking data dependency between vTensors.

GPU0 to execute operator  $op_1$ . SuperScaler records such assignment by annotating the data flow graph, which will be enforced during execution. After the assignment, the corresponding input and output tensors of the assigned operators naturally co-locate on the same device.  $op\_order(op_1, op_2)$  adds a happen-before edge in SuperScaler graph between the two operator nodes, and will perform  $op_1$  computation before  $op_2$  during execution.

**Scheduling validation and completion.** The freedom of arbitrary order specifying makes it possible that some  $op\_order$  calls violate previous  $op\_orders$  or data dependency. To avoid potential deadlock and keep scheduling plans feasible, SuperScaler performs scheduling validation as follows. First, for each pair of producer and consumer operators in the initial graph, SuperScaler performs an interaction over their vTensor masks. Non-empty intersections indicate the existence of data dependency, as shown in Figure 7. This way SuperScaler can identify all data dependencies after op transformation and scheduling. With the identified data dependencies and the “happen-before” relations as edges, SuperScaler will build a full dependency graph. And the execution scheduling is feasible only if it is an acyclic graph, which can be checked with graph circle detection algorithms [15]. In certain cases, such as replicated producers, the consumer may depend on any one of the producers. SuperScaler will enumerate these possibilities and consider the scheduling feasible if at least one acyclic graph exists. In some cases, the operator execution order on one device is unspecified, introducing ambiguity. To avoid potential deadlock due to ambiguous execution, SuperScaler specifies a feasible order for these operators by applying a topological sort [22] over the full dependency graph and returning the global sequential order.

### 3.3 Dependency Materialization

After transformation and scheduling, operators in a SuperScaler graph may have some upstream output vTensor mismatched its downstream input vTensor, or located in different devices. Data dependency materialization fixes these problems with the following steps.

First, the non-empty overlapped portion of producer and consumer vTensors are identified by intersecting the masks

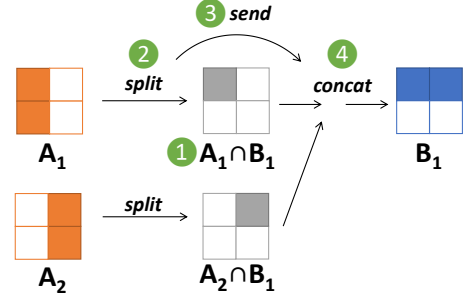


Figure 8: Data dependency materialization for producer vTensors  $A_1, A_2$  and consumer vTensor  $B_1$ .

in both vTensors. Second, for the produced vTensor, a split operator is inserted to extract the overlapped portion of the two vTensors. A pair of send-recv operators will be inserted if the two vTensors locate in different devices. Finally, a concat or reduce operator on the consumer side is inserted to construct an input vTensor with the desired shape from multiple producers. Figure 8 illustrates an example of data dependency materialization. Operators  $A_1$  and  $A_2$  produce the left and right half of the tensor and operator  $B_1$  consumes the top half. The overlapped regions  $A_1 \cap B_1$  and  $A_2 \cap B_1$  are the top-left and top-right part, respectively ①. It then splits both  $A_1$  and  $A_2$  to extract the overlapped region ②. For cross-device tensors, communication operation will be added ③. Finally, on the receiver side, it concatenates the collected pieces as  $B_1$  ④. The changes will be recorded in the SuperScaler graph for later code generation. During materialization, there exist optimization opportunities for communications, which we elaborate in §4.

## 3.4 Exploring More Parallelization Plans

With the above design, SuperScaler can support existing popular parallelization plans as well as new flexible parallelization plans for emerging models. Note that we skip the new pipeline parallelism for AlphaFold2 and co-shard as they have been discussed in §2.

### 3.4.1 Data Parallelism

Algorithm 1 shows an example sProgram for data parallelism. It takes a SuperScaler graph and device environment as input. Each forward computation operator will be partitioned along the “batch” dimension with  $op\_trans$  (Line 3-5). The other optimizer operators will be replicated (Line 6-7). Then the transformed operators will be assigned among devices (Line 8-9). The operator type and dimension information used in `IsForward` and `GetBatchDim()` are captured from DFG and kept in SuperScaler graph (§5). Note that backward operators can be omitted in the specification, SuperScaler will adapt them to their forward operators automatically through operator transformation (§5)

---

**Algorithm 1: Data Parallelism sProgram.**

---

**Input:** SuperScalerGraph  $g$ , Environment  $env$   
**Output:** transformed SuperScalerGraph  $g$

```
1 ndevs  $\leftarrow$  |env.devices| // get device number
2 for  $op \in g.ops$  do
3   if IsForward( $op$ ) then // partition forward ops
4     dim  $\leftarrow$  GetBatchDim( $op$ )
5     new_ops  $\leftarrow$  op-trans( $op$ , SplitAlgo(dim, ndevs))
6   else // replicate optimizer ops
7     new_ops  $\leftarrow$  op-trans( $op$ , ReplicaAlgo(ndevs))
8   for new_op, device in zip(new_ops, env.devices) do
9     op-assign(new_op, device)
```

---

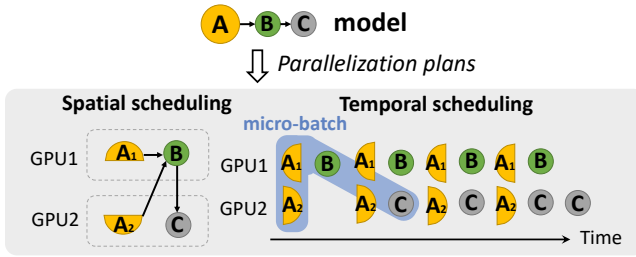


Figure 9: Interlaced pipeline scheduling.

### 3.4.2 Interlaced Pipeline Parallelism

mBART is a language translation model [29] with imbalance layers. It consists of embedding layers and transformer layers. The embedding layers consume large memory with little computation load, while the transformer layers are opposite, leading to imbalance resource utilization if organizing the layers into stages. Existing pipeline parallelisms [19, 45] can only place different stages on disjoint devices. Such parallelization plan will lead to low resource utilization due to imbalanced resource consumption across stages.

To tailor a parallelization plan for this model, we break the assumption of existing pipeline parallelisms that the stages must be placed on disjoint devices. To this end, the embedding layer as the first pipeline stage shares the devices with all other stages. Figure 9 shows an simplified imbalance model and its tailored parallelization plan. Such tailored parallelism can be considered as a regular pipeline among transformer layers, while interlaced with tensor model parallel over embedding layers, which is referred to as *Interlaced Pipeline*.

**sProgram for Interlaced Pipeline.** Interlaced Pipeline is more complex than existing pipeline parallelisms, The corresponding sProgram is shown in Algo 2. The program first transforms the graph to  $K$  micro-batches (Line 2-3). It places transformer operators (*i.e.*,  $stage\_ops$ ) to different devices (Line 6-8). Then, for embedding layers (*i.e.*,  $emb\_ops$ ), it further splits it into  $S$  partitions and places them across all devices (Line 10-13).

After operator transformation and placement, the program

---

**Algorithm 2: Interlaced Pipeline Scheduling**

---

**Input:** SuperScalerGraph  $g$ , Environment  $env$ , Micro Batch Number  $K$

```
1  $S \leftarrow$  |env.devices| // number of stages
  // ==== 1F1B Transformation
2 for  $op \in g.ops$  do
3   dim  $\leftarrow$  GetBatchDim( $op$ )
4   op-trans( $op$ , SplitAlgo(dim,  $K$ ))
5  $emb\_ops, stage\_ops \leftarrow$  Classify( $g.ops$ )
6 for  $sid \leftarrow 1$  to  $S$  do
7   ops  $\leftarrow$  GetStageOps( $stage\_ops, sid$ )
8   op-assign(ops,  $sid$ )
  // ==== Additional transformation
9 for  $op \in emb\_ops$  do
10  ops  $\leftarrow$  op-trans( $op$ , ShardEmbedAlgo( $S$ ))
11  for  $device \in 1$  to  $S$  do
12    op-assign(ops[ $device$ ],  $device$ )
  // ==== Interlaced Pipeline Scheduling
13 tasks  $\leftarrow$  OrderTo1F1B( $stage\_ops$ )
14 previous_tasks  $\leftarrow$  GetEmbedTasks( $emb\_ops, 0$ )
15 for  $step \leftarrow 1$  to  $2*(S+K-1)$  do
16   stage_tasks  $\leftarrow$  PopHeadFromTasks(tasks)
17   op-order(previous_tasks, stage_tasks)
18   previous_tasks  $\leftarrow$  stage_tasks
19   if  $step \% 2 = 0$  then
20     embed_tasks  $\leftarrow$  GetEmbedTasks( $emb\_ops, step$ )
21     op-order(stage_tasks, embed_tasks)
22     previous_tasks  $\leftarrow$  embed_tasks
```

---

works on the temporal scheduling (Line 13-22). Transformer operators (*i.e.*,  $stage\_ops$ ) are firstly reordered to follow the same temporal order of 1F1B pipeline [50] into a sequence of stage tasks (Line 13). Then inside a “for” loop,  $op\_order$  is applied to determine such sequential temporal ordering (Line 15-18). Embedding operators (*i.e.*,  $embed\_tasks$ ) are inserted as barriers among transformer operators when the  $step$  is a multiple of 2 (Line 19-22).

Across all the above examples and other sProgram we implemented, we find decoupled primitives of  $op\_trans$ ,  $op\_assign$  and  $op\_order$  are expressive enough to cover all parallelization plans (§6).

## 4 Communication Optimization

The more flexible parallelization plans may introduce more diverse and unconventional communication patterns. During data dependency materialization, SuperScaler optimizes communications in the following ways.

**Aligning with efficient communication collectives.** Modern communication libraries [2, 16, 25] usually provide highly efficient, MPI-like collective communication interfaces, *e.g.*, broadcast, gather, reduce and all-reduce, which often outperform the peer-to-peer send and receive interfaces. Hence Su-

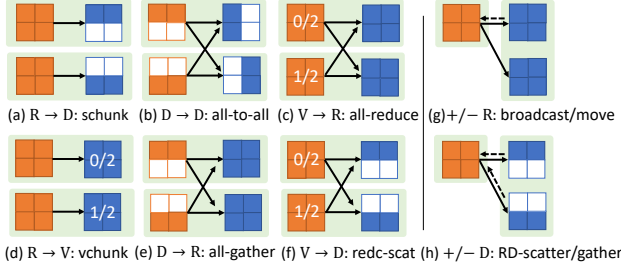


Figure 10: Communication collectives as RVD transitions. A shaded area in (a) to (f) indicates a device. A shaded part in (g) and (h) indicates a device group.

perScaler analyzes the data dependency graph and performs a pattern match to replace a group of peer-to-peer communications into high-performance collectives.

For complex communication patterns that cannot match any single interface, we design an algorithm to compose the communication with multiple communication primitives based on RVD representation.

**RVD representation.** DNN clusters are usually equipped with homogeneous accelerator devices [59]. Therefore, most parallelization plans partition operators evenly. Thus, their input or output tensors can be simply expressed as: 1)  $R(i)$ , the tensor is replicated to  $i$  copies; 2)  $V(j)$ , value split, the tensor is decomposed to  $j$  copies with the same shape; 3)  $D(k_1, k_2, \dots, k_n)$ , uniformly partition the tensor into  $k_1$  parts in the first dimension,  $k_2$  parts in the second dimension, so on so forth. We use RVD to denote the transformation of a tensor. For example,  $R(1)V(2)D(1,2)$  indicates a 2-D pTensor requires no replication, is decomposed into 2 vTensors with the same shape, and each is partitioned into 2 vTensors by partitioning the second axis. Thus,  $R(1)V(2)D(1,2)$  can represent 4 vTensors. RVD can represent both producer vTensors and consumer vTensors as they are both transformed from the pTensor.

**Communication primitive search over RVD graph.** Applying a communication primitive essentially turns an RVD to another, with a specific element-wise value exchange pattern (e.g., all-to-all or all-reduce). Thus, a communication primitive defines an RVD transition rule. Figure 10(a - f) lists communication primitives with producers and consumers on the same group of devices, which can be translated into the value changes between R, V, and D ( $i/j$  in box indicating value split into  $j$  parts and this is  $i$ -th part). With the transition rules for different communication primitives as edges, we build an RVD transition graph, and turn the communication composing problem into a problem to find a path from the producer RVD to the consumer RVD. Figure 11 shows an example that connects the producer  $R(1)V(2)D(1,2)$  to the consumer  $R(2)V(1)D(2,1)$ . It first performs an all-reduce over every 2 tensors to turn  $V(2)$  into  $R(2)$ , and gets  $R(2)V(1)D(1,2)$ . Then with an all-to-all applied on every two tensors, it converts

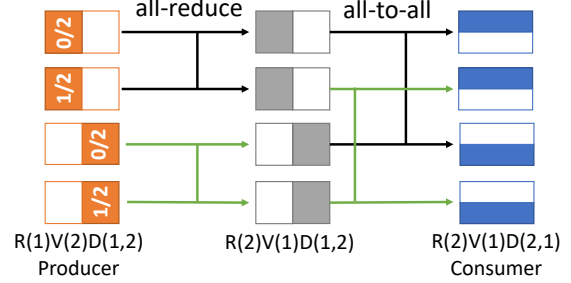


Figure 11: RVD transition path as a dependency materialization plan for an example 2D tensor communication. Arrows with different colors denote different communication groups.

$R(2)V(1)D(1,2)$  into  $R(2)V(1)D(2,1)$ . The above solution targets consumer and producer located in the same group of devices, namely intra-device-group RVD, or intra-RVD for short. It's also possible that producers and consumers locate on different groups of devices, namely inter-RVD. For inter-RVD, it first follows the above procedure to build RVD graphs for consumers and producers, respectively. Then it connects the 2 RVD graphs with extended primitives in Figure 10(g - h) as cross-graph edges, and forms a larger graph. We assign the edge weight with the time of the communication primitive and leverage Dijkstra [7] algorithm to search the shortest path from producer RVD to consumer RVD, and translate the path into a sequence of communication primitives.

This approach can accommodate new communication primitives by formulating a new RVD transition graph.

## 5 Implementation

We implement SuperScaler on top of PyTorch [36] with 18k lines of python code.

**Converting to SuperScaler graph.** We capture the computation graph using TorchScript [49]. Since TorchScript only captures forward graph, we complete it with corresponding backward nodes when converting to SuperScaler graph. For convenience, SuperScaler also tracks operator types and infers tensor shapes from DFG to support functions like `IsForward()` and `GetBatchDim()` in sProgram.

**Autograd for forward operator transformation.** We followed chain rule [42] in backward propagation to infer the correct mapping of gradient vTensors. For example, different operators consuming the same vTensor leads to the value-partition of its gradient, which will incur all-reduce for synchronization. With this ability, SuperScaler can automatically transform backward operators by inferring the gradient vTensors when transforming the corresponding forward operators.

**Op-trans assistant.** Defining transformation algorithms for all kinds of operators in DNN models requires lots of engineering effort. Inspired by Einops [41], we apply annotations on tensor dimensions to indicate transformation strategies. The

Categories	Mechanisms	Support
SPMD Parallelism	Data Parallelism [1]	✓
	Sequence Parallelism [24]	✓
	Transformer Parallelism [45]	✓
	DAP [11]	✓
	ZeRO [38]	✓
	Sequence Parallelism [26]	✓*
	Flexible Tensor Parallel [20, 53, 56]	✓
MPMD Parallelism	1F1B [45, 50]	✓
	GPipe [19]	✓
	Chimera [27]	✓
	PipeDream (Async) [33]	×
	Terapipe [28]	×
Memory Optimizations	Gradient Accumulation [54]	✓
	Recompute [10]	✓
	Chain-recompute [23]	✓
	Swap [18]	✓
Overlapping	ByteScheduler [35]	×
	All-reduce Overlap [43]	✓*

Table 1: The support to existing parallelization plans. ‘\*’ denotes additional co-scheduling of computation and communication on system level. Otherwise, the supported parallelisms can be exactly specified by sProgram.

annotation is enhanced with keywords to indicate whether a tensor can be partitioned spatially or numerically (value split).

**Code generation.** To generate code given a SuperScaler graph, the system should specify initial tensor allocation (*e.g.*, for model weights). By default, partitioned weights are initialized to co-locate with its operators. We also allow system experts to specify the initial placement of a part of weights with the tensor slicing interfaces. During code generation, we also insert memory-releasing operations, *i.e.*, free a python variable, by inspecting tensor life-cycles in the execution plan, which is necessary for inference part to save memory.

**Supported parallelization plans.** Table 1 summarizes our support to existing parallelization rules. SuperScaler is able to support 15 out of 18 plans. In addition to parallelisms, SuperScaler also supports memory optimization techniques such as recompute and swap useful in a parallelization plan. For example, swap can be achieved by an `op-trans` that inserts an identity operator before and `op-assign` to CPU. SuperScaler by design requires transformation and scheduling to respect the model semantic strictly, thus does not support asynchronous execution in PipeDream. SuperScaler captures graph from one training iteration, thus cannot support cross-iteration scheduling in ByteScheduler [35]. SuperScaler doesn’t access concrete value in tensors, thus cannot figure out data dependency at token level (*i.e.*, from a masked tensor) in Terapipe. We will investigate the support of these parallelisms in future work.

## 6 Evaluation

We compare with multiple baseline DNN training systems over diverse real-world models, to demonstrate how SuperScaler unleashes performance with new parallelization plans. Besides end-to-end performance (§6.2), we also analyze the improved memory usage (§6.3), computation efficiency (§6.4) and the highly efficient communication generated automatically (§6.5).

### 6.1 Experimental Setup

**Machine configurations.** Our evaluation is performed on a cluster with 32 NVIDIA Tesla V100 (32GB) GPUs. Each server is equipped with 8 GPUs which are connected via NVLink [3]. Servers are interconnected with 100 Gbps InfiniBand network. All the servers are installed with NCCL 2.10 [2] and PyTorch v1.11.0 [36].

**DNN models.** We evaluate system performance with four emerging models from diverse domains, including vision, natural language and biology analysis. 1) Swin-Transformer [30] is a popular vision model stacked with heterogeneous transformer layers. We set the resolution of input images to  $1536 \times 1536$ , the highest in the paper [30]. 2) GPT-3 [8] is a language model with homogeneous transformer layers. As longer sequences generally perform better [6, 12], we evaluate GPT-3 for long document tasks with input sequence length of 16384 following LongFormer [6]’s setting. 3) mBART [29] is a multilingual encoder-decoder model which has a large embedding layer to serve multiple languages in one model. We set input sequence length to 1024 (the default value), and choose the datasets with 500k vocabularies [60]. 4) AlphaFold2 [21] is a biological model for predicting protein structures, which has multiple homogeneous evoformer layers. We set input with 128 sequences and 256 residues following [21], and take a typical training setting: three forward pass and one backward pass in each iteration.

**Baseline parallel training systems.** We compare SuperScaler with four parallel DNN training systems: 1) Megatron-LM [34] (v3.0.2) is designed to train transformer-based model, which hierarchically combines pipeline-parallelism with data-/tensor-parallelisms. It evenly partitions model layers into pipeline stages, with all operators in a stage sharing the same data-/tensor-parallelism setting. 2) Alpa [61] (v0.1.5) further allows pipeline stages with different data-/tensor-parallelism settings, and employs a search algorithm to set each stage. Among the emerging DNN models we evaluated, GPT-3 is officially supported by Alpa. So, we focus the comparison between SuperScaler and Alpa on GPT-3. For other Alpa officially supported models, SuperScaler can follow its search result to build parallelization plans and achieves similar performance. 3) DeepSpeed [38] (v0.7.4) applies ZeRO [37, 39] optimizations on data parallelism to save memory. The highest level memory optimization configuration, ZeRO-3, is not



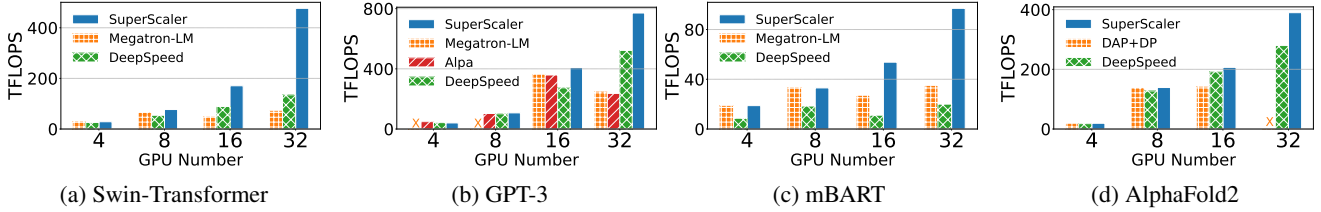


Figure 12: End-to-end evaluation. × denotes the failure of training due to out-of-memory.

Model	Parameters	Layer Number	Hidden Size	Head Number
Swin-Transformer [30]	{1.8B, 6.6B, 13B, 30B}	{32, 48, 56, 64}	{512, 768, 1024, 1536}	{16, 24, 32, 32}
GPT-3 [8]	{1.3B, 2.6B, 6.7B, 15B}	{24, 32, 32, 48}	{2048, 2560, 4096, 5120}	{32, 32, 32, 32}
mBART [29]	{4.7B, 9.5B, 20B, 32B}	{24, 32, 48, 56}	{3072, 4096, 5120, 6144}	{16, 32, 32, 32}
AlphaFold2 [21]	{87M, 930M, 2.4B, 3.2B}	{48, 64, 96, 128}	{256, 512, 1024, 1024}	{8, 16, 32, 32}

Table 2: Model architecture with increasing number of GPUs. M: million. B: billion.

compatible with pipeline parallelism. Therefore, we resort to its compatible tensor-parallelism and ZeRO data-parallelism. As ZeRO-Offload [39] memory optimization introduces expensive CPU-GPU communication overhead, we enable it only when memory is insufficient under ZeRO-3. 4) Dynamic Axial Parallelism (DAP) [11] is a tailored tensor parallelism for AlphaFold2 that partitions the input tensor along a non-batch dimension while replicating weight tensors. We combine DAP with data parallelism (DAP+DP) as baseline for AlphaFold2. Hyper-parameters, *e.g.*, parallelism size and micro-batch size, significantly affect training performance. For a fair comparison, in each evaluation, we tune hyper-parameters for each system to get their optimal settings as baseline. We also enable recompute [10] to save memory only when necessary.

## 6.2 End-to-end Performance

**SuperScaler parallelization plans.** SuperScaler enables us to apply new parallelization plans over DNN models to improve performance, including co-shard (§2), interlaced pipeline (§3.4.2) and 3F1B pipeline schedule (§2). For Swin-Transformer and GPT-3, we apply co-shard to partition attention heads and feedforward [52] hidden dimensions. For GPT-3, it is applied to every transformer layer. For Swin-Transformer, it is only applied to the first four transformer layers which consume the most memory. For mBART, we replace the original 1F1B pipeline with our interlaced pipeline. For AlphaFold2, we use the 3F1B pipeline scheduling.

We perform weak scaling test to evaluate the training performance of all these models. Following the practice of Megatron [34] and Alpa [61], we expand model size with the increasingly larger number of GPUs. The batch size is set to 128 for AlphaFold2 following [21], with other models set to 512. The complete model configurations are listed in Table 2. Similar to [34, 61], we evaluate the performance in aggregated tera floating point per second (TFLOPS).

**Results of Swin Transformer and GPT-3.** Figure 12(a) and Figure 12(b) show the end-to-end training performance on Swin Transformer and GPT-3. Compared to existing baselines, SuperScaler achieves up to  $3.5\times$  speedup on Swin Transformer, and up to  $1.5\times$  speedup on GPT-3.

For Swin-Transformer, SuperScaler’s performance is similar to Megatron-LM and DeepSpeed within one server (4-GPU, 8-GPU). This is because the high bandwidth NVLink within a server makes communication difference negligible on both systems, marginalizing SuperScaler’s communication improvement. DeepSpeed also has a similar performance due to the small model size compared to its heavy computation cost, which can easily overlap with the weight synchronization communication. On multiple servers (16-GPU, 32-GPU), SuperScaler achieves up to  $6.6\times$  and  $3.5\times$  over Megatron-LM and DeepSpeed, respectively. That is because Megatron’s tensor-parallelism requires more GPUs to fit the larger model size in memory, leading to more communication costs. With co-shard, SuperScaler achieves similar memory usage with less GPUs, showing better performance with reduced tensor-parallelism communication cost. For example, Megatron-LM requires at least 16-way tensor parallelism in the 16-GPU Swin Transformer test, while SuperScaler only needs a 4-way tensor-parallelism to fit in model, and uses communication efficient 4-way pipeline-parallelism to connect these 4-GPU tensor-parallelism groups. Similarly, in the 32-GPU test, Megatron-LM requires 32-way tensor parallelism while SuperScaler only needs 8-way.

With the reduced memory usage, DeepSpeed also requires less GPUs and outperforms Megatron-LM for similar reason. However, compared to SuperScaler, DeepSpeed still suffers from the extra communication cost due to weights and gradients synchronization.

For the similar reason on Swin-Transformer, on GPT-3, SuperScaler achieves up to  $3.3\times$  speedup over Alpa and up to  $1.5\times$  speedup over DeepSpeed. For example, we find both

Megatron-LM and Alpa need at least 16-way tensor parallelism for 15B model, while SuperScaler and DeepSpeed are able to train with 8-way tensor parallelism. Megatron-LM and Alpa achieve similar performance, which also aligns to the results in their work [61].

**mBART results.** In Figure 12(c), SuperScaler achieves up to  $2.8\times$  and  $4.9\times$  performance speedup over Megatron-LM and DeepSpeed, respectively. For 4-GPU and 8-GPU cases, SuperScaler has the same performance as Megatron-LM, which is because both of them end up with the same parallelization plans, *i.e.*, pure tensor parallelism due to memory constraints. When model size grows, the embedding layers’ weights can no longer fit within a server given tensor parallelism. Megatron-LM shows worse performance in such cases. It requires the transformer layers co-located with embedding layers must share the same tensor parallelism configuration, which introduces significant communication overheads in transformer layers. Instead, SuperScaler only partitions embedding layers across servers, while allows other layers to use within-server tensor parallelism, thus saves expensive inter-server communication. We find DeepSpeed consistently performs less efficiently than Megatron-LM or SuperScaler. That’s because DeepSpeed enables offload, which requires expensive communication to fetch large weights from CPU and synchronize large embedding gradients. And such communication can hardly overlap with computation.

**AlphaFold2 results.** In Figure 12(d), SuperScaler achieves up to  $1.4\times$  (32-GPU) speedup over baselines with the new 3F1B pipeline scheduling. When model size is small, all systems use data parallelism and therefore performs similarly. With the larger model size, both model weights and activations (*i.e.*, tensors that between two consecutive forward operators) consume more memory. DAP+DP has to use DAP to partition activations across devices to save memory, which introduces high communication costs and fails to train 3.2B model even with 32-way DAP. Instead, SuperScaler leverages 3F1B to partition model weights across devices, which only requires little communication at the boundary of pipeline stages. For example, DAP+DP requires at least 4-way DAP to train the model for 2.4B model, while SuperScaler is able to switch from DAP to 4-way 3F1B pipeline scheduling and outperform DAP+DP with  $1.5\times$  speedup on 2.4B model. DeepSpeed can also save memory on weights, but it introduces more overheads by synchronizing weights and gradients than 3F1B scheduling when GPU number is large.

### 6.3 Reducing Memory with Decoupling

The decoupling of transformation and scheduling allows parallelization plans to have more flexible scheduling choices of a same transformation, such as reducing memory usage to support training with larger models or larger data samples. To demonstrate this, we take co-shard as an example to compare with recompute and ZeRO3-Offload. Both recom-

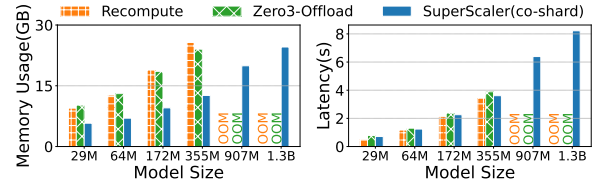


Figure 13: Swin Transformer single-GPU memory consumption and latency with growing model size.

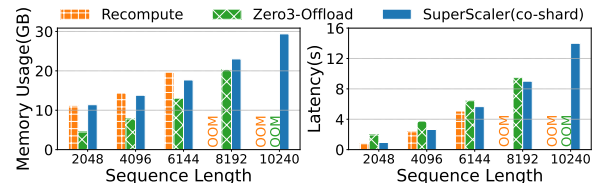


Figure 14: GPT-3 single-GPU memory consumption and latency with growing input size (sequence length).

pute and ZeRO3-Offload are memory-saving techniques. All mechanisms apply recompute for each layer. For co-shard, we additionally apply it to attention and feedforward operators. For ZeRO3-Offload, we additionally offload weight and optimizer status to CPU memory. To make fair comparisons on memory consumption, we follow the setting of global batch size 512 but fix the micro batch size to 1.

Figure 13 shows the single-GPU memory consumption and latency with the increasing model size of Swin-Transformer. With co-shard, SuperScaler can support training on single GPU with 1.3B model parameters,  $3.7\times$  the model size of ZeRO3-Offload and recompute. Compared to recompute, ZeRO3-Offload can slightly save memory on larger models, but still lead to out-of-memory (OOM.) when model size becomes large (*i.e.*, 907M and 1.3B). This is because ZeRO-Offload can only save weights and optimizer status memory, while Swin-Transformer has much larger memory consumption on activations than on weight. In contrast, co-shard effectively reduces activation memory by partitioning operators, which reduces the peak memory and hence can train larger models.

Figure 14 shows the single-GPU memory consumption and latency with the increasing input data size, *i.e.*, sequence length, of the 1.3B GPT-3 model. co-shard supports  $1.2\times$  and  $1.7\times$  the sequence length of ZeRO3-Offload and Recompute, respectively. Compared to Swin-Transformer, GPT-3 usually has relatively larger memory consumption on weights, which explains why ZeRO3-Offload saves more memory than co-shard when data size is small. However, ZeRO3-Offload’s total memory consumption grows more quickly than co-shard with the increase of sequence length, and reaches OOM at the sequence length of 10240. In contrast, co-shard has less memory consumption growth rate, and can train with the sequence length of 10240.

Considering the cost of saving memory by co-shard and

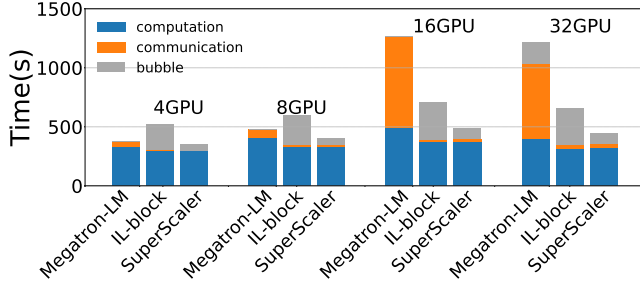


Figure 15: mBART end-to-end performance breakdown.

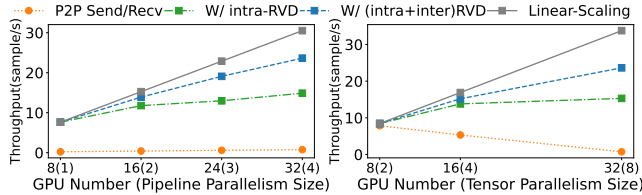


Figure 16: GPT-3 performance with growing pipeline parallelism size (left) and growing tensor parallelism size (right).

ZeRO3-Offload, we find co-shard breaks large operators into smaller ones, which may lead to less execution efficiency on GPU. However, such impact only slightly slows down the latency, as the model size or input data is large enough to saturate computation. For ZeRO3-Offload, it still suffers from communication overheads when more GPUs are involved, as we observed in §6.2.

## 6.4 Improving Efficiency with Co-Scheduling

The flexible space-time co-scheduling allows SuperScaler to explore new parallelization plans for better resource utilization, *e.g.*, interlaced pipeline. We perform a breakdown analysis on mBART to demonstrate how interlaced pipeline improves resource utilization with less idle time and more balanced resource consumption.

We profile the end-to-end training and compare SuperScaler with Megatron-LM and Interlaced-block (IL-block). IL-block stands for the interlaced-pipeline scheduling but with the conventional more coarse-grained recompute scheduling. The end-to-end time consists of averaged computation time, communication time and bubble time. Bubble time refers to the device idle time, *e.g.*, a stage waiting for data arrival in pipeline parallelism. Figure 15 shows the time distribution.

IL-block achieves up to  $1.9\times$  performance speedup over Megatron-LM. The performance gain mainly comes from reduced communication. For 16-GPU and 32-GPU cases, Megatron-LM spends 60% and 50% of the total time on expensive cross-server tensor parallelism communication. In contrast, interlaced-pipeline scheduling only applies cross-server tensor parallelism on embedding layers instead of all layers, which significantly reduces communication cost.

Producers	Consumers	Config. (i→j)
$\mathbf{R(i)V(1)D(1)}$	$\mathbf{R(j)V(1)D(1)}$	8→8, 8→4, 4→8
$\mathbf{R(i)V(1)D(1)}$	$\mathbf{R(1)V(1)D(j)}$	8→8, 8→4, 4→8
$\mathbf{R(1)V(i)D(1)}$	$\mathbf{R(j)V(1)D(1)}$	8→8, 8→4, 4→8
$\mathbf{R(1)V(i)D(1)}$	$\mathbf{R(1)V(1)D(j)}$	8→8, 8→4, 4→8
$\mathbf{R(1)V(1)D(i)}$	$\mathbf{R(j)V(1)D(1)}$	8→8, 8→4, 4→8
$\mathbf{R(1)V(1)D(i)}$	$\mathbf{R(1)V(1)D(j)}$	8→8, 8→4, 4→8

Table 3: The 18 cases of 6 categories for RVD search benchmark (1-D tensor).

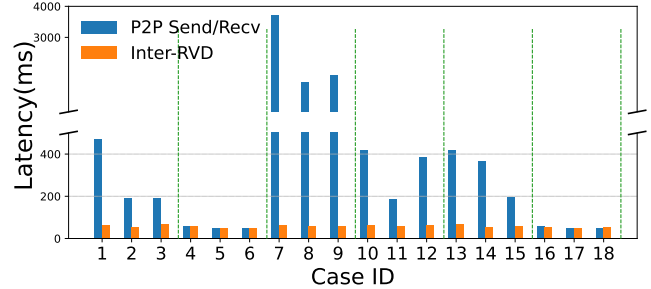


Figure 17: Inter-RVD latency on different cases.

Compared to Interlaced-block, SuperScaler can achieve another  $1.5\times$  speedup by reducing the bubble time. This is because in Interlaced-block, conventional recompute scheduling treats forward and its backward as a large operator in scheduling, which introduces an unnecessary dependency between the previous backward operation and the forward operation. This leads to the bubble time in the forward operation, waiting for the arrival of gradients. In contrast, SuperScaler by design follows the fine-grained data dependencies without such unnecessary dependency, which automatically makes the recomputing of forward operation to execute concurrently with previous backward operations. Hence it reduces the GPU idle time and leads to better efficiency.

## 6.5 Serving Diverse Communication Patterns

The flexibility in scheduling may introduce more diverse communication patterns. To evaluate the efficiency of generated communication plans with the RVD representation, we first show the end-to-end training performance of GPT-3 model optimized by intra-RVD and inter-RVD. Then we use micro benchmarks to analyze communication latency of various operator transformation strategies.

**End-to-end GPT-3 training.** We use strong scaling to test performance on the 1.3B GPT-3 model. We start from using general P2P send/recv (§3.3) as baseline, then apply with intra-RVD and inter-RVD step by step. Figure 16 shows the scalability of training throughput with the growing number of GPUs using: (left) pipeline parallelism (*i.e.*, communication message size fixed) and (right) growing tensor parallelism size (*i.e.*, communication message size increasing), respectively.

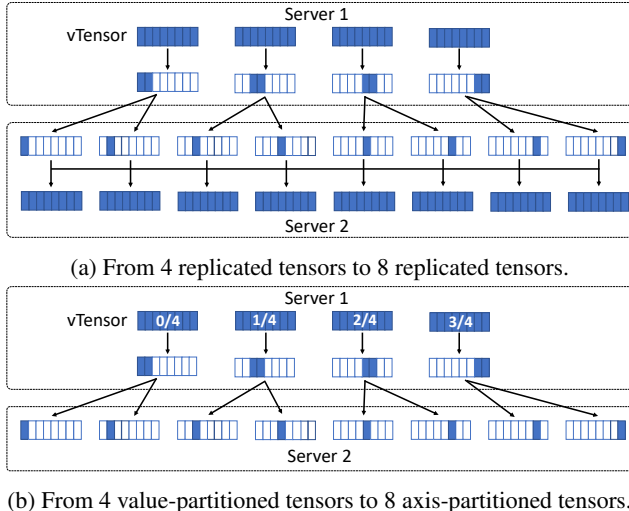


Figure 18: Two searched cases in inter-RVD.

Intra-RVD significantly outperforms P2P send/recv with up to  $32\times$  speedup when involving more GPUs (i.e., 32). Inter-RVD further improves scalability with up to  $1.6\times$  speedup, which is due to reduced cross-server communication costs.

**RVD search micro-benchmark.** To evaluate communication search on an RVD graph, we build a micro-benchmark. As intra-RVD can be viewed as a subset of inter-RVD, we perform inter-RVD search by allocating different numbers of producers on a server, and different numbers of consumers on another server. Table 3 lists the configurations of producer RVD and consumer RVD. Figure 17 shows the communication latency compared to P2P send/recv solution. Inter-RVD can improve P2P send/recv in 12 out of 18 cases, and achieves up to  $57\times$  speedup. This is because inter-RVD searches communication plans minimize the cost that considers both link bandwidth and communication volume.

**Case study.** SuperScaler is able to automatically find highly efficient communication plans like manually optimized ones in Alpa and Megatron-LM. Figure 18(a) shows a plan of transferring 4 replicated tensors in Server1 to 8 replicated tensors required by Server2. The replicated tensors in Server1 will be partitioned alongside one spatial dimension using `schunk` (Figure 10(a)), and then performs `RD-scatter` (Figure 10(h)) to scatter the sub-tensors to devices on Server2. Finally, Server2 performs an `all-gather` to gather all tensors. Instead of directly broadcasting tensors inside Server1 to Server2, which is exactly the way of P2P send/recv, RVD search identifies such a pattern due to the low bandwidth across servers, which benefits more by minimizing the communication volume across servers. A similar optimization can be found in [34]. Figure 18(b) shows another plan of transferring 4 value-partitioned tensors to 8 axis-partitioned tensors. Similarly, inter-RVD generates efficient communication plans by first performing `reduce-scatter` inside Server1, and then using `RD-scatter` to send sub-tensors to Server2.

## 7 Related Work

**Parallel DNN training.** Recently, data, tensor, and pipeline parallelisms [1, 19, 27, 37, 50] have been widely used in distributed DNN training. In addition, various memory optimizations [10, 18, 23] have been adopted to exploit large-scale model training under GPU memory constraints. Recently, systems, e.g., Megatron-LM [24, 34, 45], DeepSpeed [38], Piper [46], Unity [51] and Alpa [61], combine multiple parallelisms and memory optimizations within one system to accelerate distributed DNN training. However, these solutions fall short in relying on empirical parallelism configurations and having limited execution scheduling choices. Thus, despite their successful applications on existing training workloads, they still fail to fully utilize the hardware capabilities. In contrast, SuperScaler provides a different angle of parallelization, which breaks the building block from predefined parallelisms into fine-grained transformation and scheduling primitives. Thus, SuperScaler is able to support more flexible and efficient parallelization plans, which are considerably crucial for emerging DNN models.

**Distributed tensor abstraction and communication.** To offer programmability for parallel execution, distributed tensor abstraction [47, 48, 57] is introduced to annotate tensors with partitioning strategies and device mappings, often combined with data or tensor parallelism. However, tensors partitioning annotations only label transformation on operators, thus cannot express further flexible scheduling among partitioned parts. SuperScaler incorporates transformed vTensor and operators, allowing flexible space-time scheduling, while keeping data dependency tracking. Furthermore, various communication methods need to be injected between two consecutive operators when they operate on tensors with different partitioning methods. Due to their empirical parallelisms, systems like Mesh-TensorFlow [44], tofu [53], FlexFlow [20] and Megatron [34] rely on a few rules to generate such required communication methods. GSPMD [56], OneFlow [57] and [40, 62] additionally investigate communications for different tensor partitioning in pipeline parallelism. However, they cannot fully satisfy SuperScaler’s demand given its numerous types of transformation and arbitrary scheduling.

**Parallelization plan search.** To improve the training performance with combined parallelisms, DNN systems [17, 20, 32, 46, 53, 58, 61] using different searching techniques to find efficient parallelism configurations. Most recently, Alpa [61] leverages both integer programming and dynamic programming solvers. SuperScaler is a parallelization plan engine that focus on expanding the parallelization space beyond combined parallelisms, and complementary to above algorithms.

There are some other systems that can work together with SuperScaler, including DNN execution systems like Pathways [5] and on device execution compilers [9, 31, 55].

## 8 Conclusions

SuperScaler is a generation engine of parallelization plans used for parallel deep learning training. We observe that existing training systems rely on empirical parallelization plans, which jointly consider multiple intertwined factors at the same time. This practice shows limited flexibility and leads to the exclusion of promising parallelization plans. To overcome this, SuperScaler decouples the intertwined factors of model partitioning, scheduling, and data dependency preserving and enables the expression of highly flexible parallelization plans. As a result, SuperScaler can not only support existing popular parallelization plans, but also explore new ones that significantly improve the training performance of emerging models as well as well-optimized large language models.

## References

- [1] Distributed Data Parallelism. <https://pytorch.org/docs/stable/notes/ddp.html>. [Online; accessed Sep.-2022].
- [2] NVIDIA collective communications library. <https://developer.nvidia.com/nccl>. [Online; accessed Aug.-2021].
- [3] NVIDIA NVLINK. <http://www.nvidia.com/object/nvlink.html>.
- [4] Martín Abadi, Paul Barham, Jianmin Chen, Zhifeng Chen, Andy Davis, Jeffrey Dean, Matthieu Devin, Sanjay Ghemawat, Geoffrey Irving, Michael Isard, et al. Tensorflow: A system for large-scale machine learning. In *OSDI*, volume 16, pages 265–283, 2016.
- [5] Paul Barham, Aakanksha Chowdhery, Jeff Dean, Sanjay Ghemawat, Steven Hand, Daniel Hurt, Michael Isard, Hyeontaek Lim, Ruoming Pang, Sudip Roy, et al. Pathways: Asynchronous distributed dataflow for ml. *Proceedings of Machine Learning and Systems*, 4:430–449, 2022.
- [6] Iz Beltagy, Matthew E Peters, and Arman Cohan. Longformer: The long-document transformer. *arXiv preprint arXiv:2004.05150*, 2020.
- [7] John Adrian Bondy, Uppaluri Siva Ramachandra Murty, et al. *Graph theory with applications*, volume 290. Macmillan London, 1976.
- [8] Tom B Brown, Benjamin Mann, Nick Ryder, Melanie Subbiah, Jared Kaplan, Prafulla Dhariwal, Arvind Nee-lakantan, Pranav Shyam, Girish Sastry, Amanda Askell, et al. Language models are few-shot learners. *arXiv preprint arXiv:2005.14165*, 2020.
- [9] Tianqi Chen, Thierry Moreau, Ziheng Jiang, Lianmin Zheng, Eddie Yan, Haichen Shen, Meghan Cowan, Leyuan Wang, Yuwei Hu, Luis Ceze, et al. Tvm: An automated end-to-end optimizing compiler for deep learning. In *13th USENIX Symposium on Operating Systems Design and Implementation (OSDI 18)*, pages 578–594, 2018.
- [10] Tianqi Chen, Bing Xu, Chiyuan Zhang, and Carlos Guestrin. Training deep nets with sublinear memory cost. *arXiv preprint arXiv:1604.06174*, 2016.
- [11] Shenggan Cheng, Ruidong Wu, Zhongming Yu, Binrui Li, Xiwen Zhang, Jian Peng, and Yang You. Fastfold: Reducing alphafold training time from 11 days to 67 hours. *arXiv preprint arXiv:2203.00854*, 2022.
- [12] Rewon Child, Scott Gray, Alec Radford, and Ilya Sutskever. Generating long sequences with sparse transformers. *arXiv preprint arXiv:1904.10509*, 2019.
- [13] Aakanksha Chowdhery, Sharan Narang, Jacob Devlin, Maarten Bosma, Gaurav Mishra, Adam Roberts, Paul Barham, Hyung Won Chung, Charles Sutton, Sebastian Gehrmann, et al. Palm: Scaling language modeling with pathways. *arXiv preprint arXiv:2204.02311*, 2022.
- [14] Jacob Devlin, Ming-Wei Chang, Kenton Lee, and Kristina Toutanova. Bert: Pre-training of deep bidirectional transformers for language understanding. *arXiv preprint arXiv:1810.04805*, 2018.
- [15] Shimon Even. *Graph algorithms*. Cambridge University Press, 2011.
- [16] Richard L Graham, Timothy S Woodall, and Jeffrey M Squyres. Open mpi: A flexible high performance mpi. In *International Conference on Parallel Processing and Applied Mathematics*, pages 228–239. Springer, 2005.
- [17] Ubaid Ullah Hafeez, Xiao Sun, Anshul Gandhi, and Zhenhua Liu. Towards optimal placement and scheduling of dnn operations with pesto. In *Proceedings of the 22nd International Middleware Conference*, pages 39–51, 2021.
- [18] Chien-Chin Huang, Gu Jin, and Jinyang Li. Swapadvisor: Pushing deep learning beyond the gpu memory limit via smart swapping. In *Proceedings of the Twenty-Fifth International Conference on Architectural Support for Programming Languages and Operating Systems*, pages 1341–1355, 2020.
- [19] Yanping Huang, Youlong Cheng, Ankur Bapna, Orhan Firat, Dehao Chen, Mia Chen, HyoukJoong Lee, Jiquan Ngiam, Quoc V Le, Yonghui Wu, et al. Gpipe: Efficient training of giant neural networks using pipeline parallelism. In *Advances in Neural Information Processing Systems*, pages 103–112, 2019.

- [20] Zhihao Jia, Matei Zaharia, and Alex Aiken. Beyond data and model parallelism for deep neural networks. *SysML 2019*, 2019.
- [21] John Jumper, Richard Evans, Alexander Pritzel, Tim Green, Michael Figurnov, Olaf Ronneberger, Kathryn Tunyasuvunakool, Russ Bates, Augustin Židek, Anna Potapenko, et al. Highly accurate protein structure prediction with alphafold. *Nature*, 596(7873):583–589, 2021.
- [22] Arthur B Kahn. Topological sorting of large networks. *Communications of the ACM*, 5(11):558–562, 1962.
- [23] Marisa Kirisame, Steven Lyubomirsky, Altan Haan, Jennifer Brennan, Mike He, Jared Roesch, Tianqi Chen, and Zachary Tatlock. Dynamic tensor rematerialization. In *9th International Conference on Learning Representations, ICLR 2021, Virtual Event, Austria, May 3-7, 2021*. OpenReview.net, 2021.
- [24] Vijay Korthikanti, Jared Casper, Sangkug Lym, Lawrence McAfee, Michael Andersch, Mohammad Shoeybi, and Bryan Catanzaro. Reducing activation recomputation in large transformer models. *arXiv preprint arXiv:2205.05198*, 2022.
- [25] Shen Li, Yanli Zhao, Rohan Varma, Omkar Salpekar, Pieter Noordhuis, Teng Li, Adam Paszke, Jeff Smith, Brian Vaughan, Pritam Damania, et al. Pytorch distributed: Experiences on accelerating data parallel training. *arXiv preprint arXiv:2006.15704*, 2020.
- [26] Shenggui Li, Fuzhao Xue, Yongbin Li, and Yang You. Sequence parallelism: Making 4d parallelism possible. *arXiv preprint arXiv:2105.13120*, 2021.
- [27] Shigang Li and Torsten Hoefler. Chimera: efficiently training large-scale neural networks with bidirectional pipelines. In *Proceedings of the International Conference for High Performance Computing, Networking, Storage and Analysis*, pages 1–14, 2021.
- [28] Zhuohan Li, Siyuan Zhuang, Shiyuan Guo, Danyang Zhuo, Hao Zhang, Dawn Song, and Ion Stoica. Terapipe: Token-level pipeline parallelism for training large-scale language models. In *International Conference on Machine Learning*, pages 6543–6552. PMLR, 2021.
- [29] Yinhan Liu, Jiatao Gu, Naman Goyal, Xian Li, Sergey Edunov, Marjan Ghazvininejad, Mike Lewis, and Luke Zettlemoyer. Multilingual denoising pre-training for neural machine translation. *Transactions of the Association for Computational Linguistics*, 8:726–742, 2020.
- [30] Ze Liu, Han Hu, Yutong Lin, Zhuliang Yao, Zhenda Xie, Yixuan Wei, Jia Ning, Yue Cao, Zheng Zhang, Li Dong, et al. Swin transformer v2: Scaling up capacity and resolution. *arXiv preprint arXiv:2111.09883*, 2021.
- [31] Lingxiao Ma, Zhiqiang Xie, Zhi Yang, Jilong Xue, Youshan Miao, Wei Cui, Wenxiang Hu, Fan Yang, Lintao Zhang, and Lidong Zhou. Rammer: Enabling holistic deep learning compiler optimizations with rtasks. In *14th USENIX Symposium on Operating Systems Design and Implementation (OSDI 20)*, pages 881–897, 2020.
- [32] Yanjun Ma, Dianhai Yu, Tian Wu, and Haifeng Wang. Paddlepaddle: An open-source deep learning platform from industrial practice. *Frontiers of Data and Computing*, 1(1):105–115, 2019.
- [33] Deepak Narayanan, Aaron Harlap, Amar Phanishayee, Vivek Seshadri, Nikhil R Devanur, Gregory R Ganger, Phillip B Gibbons, and Matei Zaharia. Pipedream: generalized pipeline parallelism for dnn training. In *Proceedings of the 27th ACM Symposium on Operating Systems Principles*, pages 1–15, 2019.
- [34] Deepak Narayanan, Mohammad Shoeybi, Jared Casper, Patrick LeGresley, Mostofa Patwary, Vijay Anand Korthikanti, Dmitri Vainbrand, Prethvi Kashinkunti, Julie Bernauer, Bryan Catanzaro, et al. Efficient large-scale language model training on gpu clusters. *arXiv preprint arXiv:2104.04473*, 2021.
- [35] Yanghua Peng, Yibo Zhu, Yangrui Chen, Yixin Bao, Bairen Yi, Chang Lan, Chuan Wu, and Chuanxiong Guo. A generic communication scheduler for distributed dnn training acceleration. In *Proceedings of the 27th ACM Symposium on Operating Systems Principles*, pages 16–29, 2019.
- [36] PyTorch Team. PyTorch. <https://pytorch.org/>. [Online; accessed Mar.-2022.
- [37] Samyam Rajbhandari, Jeff Rasley, Olatunji Ruwase, and Yuxiong He. Zero: Memory optimization towards training a trillion parameter models. *arXiv preprint arXiv:1910.02054*, 2019.
- [38] Jeff Rasley, Samyam Rajbhandari, Olatunji Ruwase, and Yuxiong He. Deepspeed: System optimizations enable training deep learning models with over 100 billion parameters. In *Proceedings of the 26th ACM SIGKDD International Conference on Knowledge Discovery & Data Mining*, pages 3505–3506, 2020.
- [39] Jie Ren, Samyam Rajbhandari, Reza Yazdani Aminabadi, Olatunji Ruwase, Shuangyan Yang, Minjia Zhang, Dong Li, and Yuxiong He. Zero-offload: Democratizing billion-scale model training. In *2021 USENIX Annual Technical Conference (USENIX ATC 21)*, pages 551–564, 2021.

- [40] Norman A Rink, Adam Paszke, Dimitrios Vytiniotis, and Georg Stefan Schmid. Memory-efficient array redistribution through portable collective communication. *arXiv preprint arXiv:2112.01075*, 2021.
- [41] Alex Rogozhnikov. Einops: Clear and reliable tensor manipulations with einstein-like notation. In *International Conference on Learning Representations*, 2021.
- [42] David E Rumelhart, Geoffrey E Hinton, and Ronald J Williams. Learning representations by back-propagating errors. *nature*, 323(6088):533–536, 1986.
- [43] Alexander Sergeev and Mike Del Balso. Horovod: fast and easy distributed deep learning in tensorflow. *arXiv preprint arXiv:1802.05799*, 2018.
- [44] Noam Shazeer, Youlong Cheng, Niki Parmar, Dustin Tran, Ashish Vaswani, Penporn Koanantakool, Peter Hawkins, HyoukJoong Lee, Mingsheng Hong, Cliff Young, et al. Mesh-tensorflow: Deep learning for supercomputers. In *Advances in Neural Information Processing Systems*, pages 10414–10423, 2018.
- [45] Mohammad Shoeybi, Mostafa Patwary, Raul Puri, Patrick LeGresley, Jared Casper, and Bryan Catanzaro. Megatron-lm: Training multi-billion parameter language models using gpu model parallelism. *arXiv preprint arXiv:1909.08053*, 2019.
- [46] Jakub M Tarnawski, Deepak Narayanan, and Amar Phanishayee. Piper: Multidimensional planner for dnn parallelization. *Advances in Neural Information Processing Systems*, 34, 2021.
- [47] Google Tensorflow Team. DTensor Concepts. [https://www.tensorflow.org/guide/dtensor\\_overview](https://www.tensorflow.org/guide/dtensor_overview). [Online; accessed Dec.-2022.
- [48] PyTorch Team. PyTorch DistributedTensor (DTensor). [https://github.com/pytorch/pytorch/tree/master/torch/distributed/\\_tensor](https://github.com/pytorch/pytorch/tree/master/torch/distributed/_tensor). [Online; accessed Dec.-2022.
- [49] PyTorch Team. TorchScript. <https://pytorch.org/docs/stable/jit.html>.
- [50] Brett Trost, Ryan Arsenault, Philip Griebel, Scott Napper, and Anthony Kusalik. Dapple: a pipeline for the homology-based prediction of phosphorylation sites. *Bioinformatics*, 29(13):1693–1695, 2013.
- [51] Colin Unger, Zhihao Jia, Wei Wu, Sina Lin, Mandeep Baines, Carlos Efrain Quintero Narvaez, Vinay Ramakrishnaiah, Nirmal Prajapati, Pat McCormick, Jamaludin Mohd-Yusof, et al. Unity: Accelerating dnn training through joint optimization of algebraic transformations and parallelization. In *16th USENIX Symposium on Operating Systems Design and Implementation (OSDI 22)*, pages 267–284, 2022.
- [52] Ashish Vaswani, Noam Shazeer, Niki Parmar, Jakob Uszkoreit, Llion Jones, Aidan N Gomez, Łukasz Kaiser, and Illia Polosukhin. Attention is all you need. *Advances in neural information processing systems*, 30, 2017.
- [53] Minjie Wang, Chien-chin Huang, and Jinyang Li. Supporting very large models using automatic dataflow graph partitioning. In *Proceedings of the Fourteenth EuroSys Conference 2019*, pages 1–17, 2019.
- [54] Pijika Watcharapichat, Victoria Lopez Morales, Raul Castro Fernandez, and Peter Pietzuch. Ako: Decentralised deep learning with partial gradient exchange. In *Proceedings of the Seventh ACM Symposium on Cloud Computing*, pages 84–97, 2016.
- [55] XLA and TensorFlow teams. XLA — TensorFlow, compiled. <https://developers.googleblog.com/2017/03/xla-tensorflow-compiled.html>.
- [56] Yuanzhong Xu, HyoukJoong Lee, Dehao Chen, Blake Hechtman, Yanping Huang, Rahul Joshi, Maxim Krikun, Dmitry Lepikhin, Andy Ly, Marcello Maggioni, et al. Gspmd: General and scalable parallelization for ml computation graphs. *arXiv preprint arXiv:2105.04663*, 2021.
- [57] Jinhui Yuan, Xinqi Li, Cheng Cheng, Juncheng Liu, Ran Guo, Shenghang Cai, Chi Yao, Fei Yang, Xiaodong Yi, Chuan Wu, et al. Oneflow: Redesign the distributed deep learning framework from scratch. *arXiv preprint arXiv:2110.15032*, 2021.
- [58] Hao Zhang, Yuan Li, Zhijie Deng, Xiaodan Liang, Lawrence Carin, and Eric Xing. Autosync: Learning to synchronize for data-parallel distributed deep learning. *Advances in Neural Information Processing Systems*, 33:906–917, 2020.
- [59] Hanyu Zhao, Zhenhua Han, Zhi Yang, Quanlu Zhang, Fan Yang, Lidong Zhou, Mao Yang, Francis C.M. Lau, Yuqi Wang, Yifan Xiong, and Bin Wang. Hived: Sharing a gpu cluster for deep learning with guarantees. *OSDI’20*, 2020.
- [60] Bo Zheng, Li Dong, Shaohan Huang, Saksham Singhal, Wanxiang Che, Ting Liu, Xia Song, and Furu Wei. Allocating large vocabulary capacity for cross-lingual language model pre-training. In *Empirical Methods in Natural Language Processing*, pages 3203–3215, 2021.

- [61] Lianmin Zheng, Zhuohan Li, Hao Zhang, Yonghao Zhuang, Zhifeng Chen, Yanping Huang, Yida Wang, Yuanzhong Xu, Danyang Zhuo, Joseph E Gonzalez, et al. Alpa: Automating inter-and intra-operator parallelism for distributed deep learning. *arXiv preprint arXiv:2201.12023*, 2022.
- [62] Yonghao Zhuang, Hexu Zhao, Lianmin Zheng, Zhuohan Li, Eric P. Xing, Qirong Ho, Joseph E. Gonzalez, Ion Stoica, and Hao Zhang. On optimizing the communication of model parallelism. *CoRR*, abs/2211.05322, 2022.